CHARACTERIZATION OF $Cu(In,Ga)Se_2$ THIN FILMS USING REFLECTED SECOND HARMONIC GENERATION

G. Buinitskaya[1], L. Kulyuk[1], V. Mirovitskii[1], E. Mishina[2], N. Sherstyuk[2], and K. Ramanathan[3]

[1] *Institute of Applied Physics, Academy of Sciences of Moldova, Academiei str. 5, Chisinau, MD-2028 Republic of Moldova*

[2] *Moscow Institute of Radioengineering, Electronics and Automation, Vernadskogo ave. 78, Moscow, 119454 Russia*

[3] *National Center for Photovoltaics, National Renewable Energy Laboratory 1617 Cole Boulevard, Golden, CO 80401*

(Received 25 January 2011)

Abstract

A thin film of $CuIn_xGa_{1-x}Se_2$ obtained by physical vapor deposition on a glass substrate covered by a Mo-film has been tested by the second harmonic generation (SHG) technique. The intensity of reflected SHG has been measured as a function of rotation angle around normal to the sample surface. To reveal the preferential orientation of micro-crystals in the film, using these data, the theoretical model of SHG in a multilayered structure has been developed. In the frame of the proposed model, the Euler angles defining the orientation of optical axis of the film texture, the ratio of two constants of nonlinear susceptibility, and the effective thickness of the film were numerically calculated.

1. Introduction

The $CuIn_{1-x}Ga_xSe_2$ quaternary compounds (CIGS), due to the direct band gap in the range of 1.4-1.6 eV and fairly high values of absorption coefficient, are among the most promising materials for the production of thin-film based photovoltaic devices [1, 2].

A further development of fabrication technologies for high-quality CIGS films requires fast and cheap methods for testing their structure. A nonlinear-optical technique of the second harmonic generation (SHG) developed in [3-5] was shown to be a powerful tool for a prompt, remote, and invasive characterization of thin films. In the present paper, this technique is modified and applied for the structural characterization of CIGS polycrystalline thin films. Based on the analysis of the SHG, the anisotropy and polarization characteristics of the film texture are obtained.

2. Experimental

The investigated CIGS thin films grown on Mo-coated glass substrates were obtained at NREL using the three stage process of co-evaporation [1]. The composition ratio of the sample determined by micro X-ray structure analyzer was the following: 24% Cu, 22% In, 3% Ga, and 51% Se. Hence, it can be concluded that the sample composition is almost stoichiometric and can be presented as $Cu_{0.96}In_{0.88}Ga_{0.12}Se_{2.04}$. Taking into account the results presented in [6], the same conclusion can be drawn from the position of the maximum and of the short wavelength wing of the photoluminescence spectra (Fig. 1a) taken at 10 and 70K.

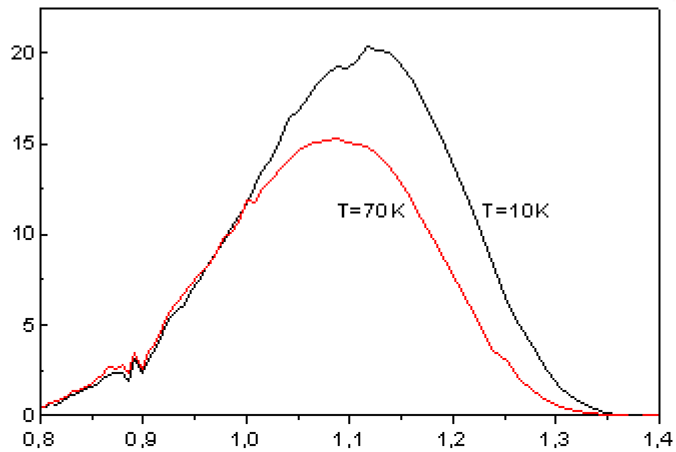

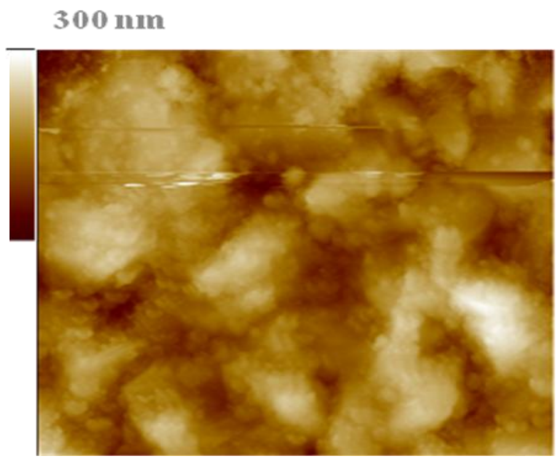

a) b)

Fig. 1. a) PL spectra of the $CuInGaSe_2$ thin film at low temperatures.
b) AFM image 5×5 μm^2 for the investigated sample.

The surface morphology of the samples was inspected by the atomic force microscope (AFM). Figure 1b shows that the sample consists of nanocrystals of a random shape with an average size in a range of 200-500 nm.

For the SHG experiments, the output of a Ti:sapphire laser was used as the fundamental radiation at 760 nm, with a pulse width of 100 fs, a repetition rate of 82 MHz, and an average power of 50 mW, focused onto a spot of about 100 μm in diameter. The angle of incidence was ϑ_i=45^o. The fundamental and the second harmonic waves were polarized both either perpendicular or in the plane of incidence (*s*-in, *s*-out or *p*-in, *p*-out polarization combinations).

The azimuthal dependences of the SHG intensity were measured in the reflection direction by rotating the sample around its normal (Fig. 2). Noting the laboratory frame as $X^{(L)}Y^{(L)}Z^{(L)}$ (in further (x, y, z)) and the film (surface) frame as $X^{(S)}Y^{(S)}Z^{(S)}$ (in further (x', y', z')), the measured azimuth angle φ corresponds to the angle between the $X^{(L)}$ and $X^{(S)}$ axes. The SHG signal in reflection geometry was spectroscopically filtered by a proper color filter and detected by a PMT and photon counting system.

Experimental azimuthal dependences $I_{2\omega}(\varphi)$ represented in Fig. 3 (dots) manifest two- or fourfold anisotropic dependences on the isotropic background. The presence of the anisotropic component in the azimuthal dependences confirms the long range ordering of nanocrystals. The strong isotropic background observed at any detection angle is caused by the presence of disorder in the system.

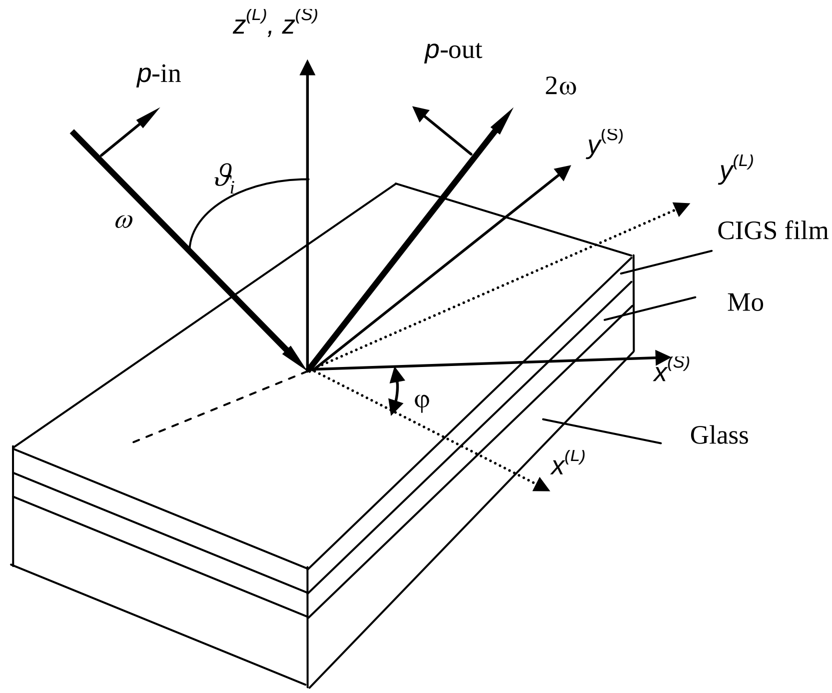

Fig. 2. Schematic of the SHG experimental geometry. The sample is rotated around the *Z*-axis; $X^{(L)}Y^{(L)}Z^{(L)}$ is the laboratory frame and $X^{(S)}Y^{(S)}Z^{(S)}$ is the film frame, φ is the azimuthal angle of the sample.

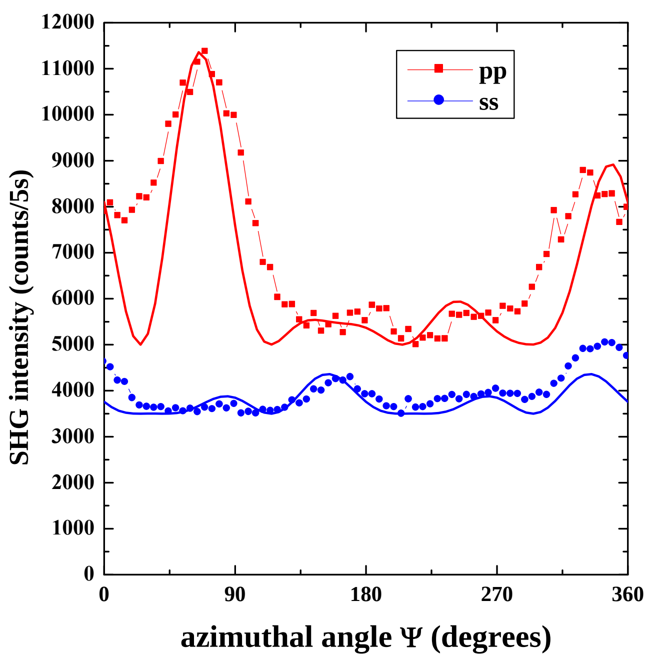

Fig. 3. SHG intensity dependences on the azimuthal angle: experimental points and fits to data (lines).

3. Theoretical Model

Bulk CIGS compounds crystallize in the chalcopyrite structure (point-group symmetry $\bar{4}2m$) [7 and references therein]. To obtain quantitative characteristics of the texture anisotropy, the measured dependence $I_{2\omega}(\varphi)$ has been analyzed by the numerical simulation of SHG-response of the nonlinear (NL) anisotropic layer. The authors have developed a theoretical model to describe the SHG "in reflection" into a multilayered structure at an arbitrary incident angle and in the direction of the fundamental light polarization. The effect of multifold reflections in each layer and light absorption, as well as the anisotropy of nonlinear optical properties of the film (sample), was taken into account. Using the proposed model, the real textured film is represented as a thin plane-parallel crystalline slab characterized by several effective parameters. These parameters are the components of the nonlinear susceptibility tensor, the effective thickness of the film, and the angles that specify the orientation of the symmetry axes of the sample with respect to the laboratory frame. All these parameters have to be determined from the comparison of the calculated pattern with the measured one. We successfully used a similar and partially simplified model to describe the texture of the transparent ZnO thin films deposited on the glass substrate [5].

Figure 2 shows the scheme of fundamental beam incident on the two-layered structure “CIGS film–Mo film” and the second harmonic beam reflected from it.The glass substrate is not taken into account, because the Mo-film is thick enough ($l \sim 1$ μm) to screen the substrate completely. Let us consider briefly the calculation of fields in the system. Only $E_y^{(\alpha)}, E_z^{(\alpha)}$, and $H_x^{(\alpha)}$ components of the electric and magnetic fields are taken into consideration at *p*-in - *p*-out polarizations (the symbol α enumerates semi-infinite media or layers: α = 0 for the air, α = 1 for the CIGS film, and α = 2 for the Mo-film). We consider those components as a superposition of the waves $E_i^{(\alpha)}$ and $E_i^{(\alpha)\prime}$ (the same is valid for the magnetic field), which propagate forwards and backwards. Each of the waves is determined by the multiple reflections of it in the complete system:

$$E_i^{(\alpha)}(y,z,\omega) = E_{i-}^{(\alpha)}(y,z,\omega) + E_{i+}^{(\alpha)}(y,z,\omega),\ i = y,z, \tag{1}$$

$$H_x^{(\alpha)}(y,z,\omega) = H_{x-}^{(\alpha)}(y,z,\omega) + H_{x+}^{(\alpha)}(y,z,\omega), \tag{2}$$

here we use the notation

$$H_{x-}^{(\alpha)}(y,z,\omega) = \boldsymbol{x}A_\alpha e^{i(K_-^\alpha r-\omega t)}, H_{x+}^{(\alpha)}(y,z,\omega) = \boldsymbol{x}B_\alpha e^{i(K_+^\alpha r-\omega t)}. \tag{3}$$

We conceive the solution to the Maxwell’s equations for the electric and magnetic fields of the second harmonic in the CIGS film as a sum of the general solution to the homogeneous wave equation and a particular solution to the inhomogeneous equation containing a distributed source of nonlinear polarization:

$$\boldsymbol{E}(2\omega) = \boldsymbol{E}_h(2\omega) + \boldsymbol{E}_{ih}(2\omega), \quad \boldsymbol{H}(2\omega) = \boldsymbol{H}_h(2\omega) + \boldsymbol{H}_{ih}(2\omega). \tag{4}$$

Our consideration here can be restricted to $E_y^{(\alpha)}(2\omega)$, $E_z^{(\alpha)}(2\omega)$ and $H_x^{(\alpha)}(2\omega)$ components, as we are interested in only *p*-out second harmonic polarization. The problem for a homogeneous contribution into the fields of the second harmonic is entirely equivalent to the corresponding problem for a fundamental beam. Therefore, we represent the x-component of the magnetic field in the form

$$H_{x,h}^{(\alpha)}(y,z,2\omega) = H_{x-}^{(\alpha)}(y,z,2\omega) + H_{x+}^{(\alpha)}(y,z,2\omega), \tag{5}$$

with $H_{x-}^{(\alpha)}(y,z,2\omega) = x \cdot F_\alpha e^{i(K_{f-}^{(\alpha)}(2\omega)r-2\omega t)}$, $H_{x+}^{(\alpha)}(y,z,2\omega) = x \cdot G_\alpha e^{i(K_{f+}^{(\alpha)}(2\omega)r-2\omega t)}$, (6)

where F_α and G_α are unknown constants to be determined.
Expressions of (5)-(6) results in the following components of the SH electric field:

$$E^{(\alpha)}_{y,z,h}(y,z,2\omega)=\left(\frac{c}{2\omega}\right)\left(\frac{K^{(\alpha)}_{fZ}(2\omega)}{\varepsilon^{(\alpha)}_{2\omega}}\right)\left(H^{(\alpha)}_{x-}(y,z,2\omega)\mp H^{(\alpha)}_{x+}(y,z,2\omega)\right) \tag{7}$$

were we use notations:

$K^{(\alpha)}_{f\pm}(2\omega)=\pm k^{(\alpha)}_f(2\omega)+iq^{(\alpha)}_f(2\omega)$, $k^{(\alpha)}_f(2\omega)=\left(\frac{2\omega}{c}\right)n^{(\alpha)}_{2\omega}$, $q^{(\alpha)}_f(2\omega)=\left(\frac{2\omega}{c}\right)\kappa^{(\alpha)}_{2\omega}$ and

$$\varepsilon^{(\alpha)}_{2\omega}=\left(\frac{c}{2\omega}\right)^2\left\{\left[\left(k^{(\alpha)}_f(2\omega)\right)^2-\left(q^{(\alpha)}_f(2\omega)\right)^2\right]+2i\,k^{(\alpha)}_f(2\omega)\,q^{(\alpha)}_f(2\omega)\right\}$$

Inhomogeneous contribution to the electric field can be represented as

$$\begin{aligned}E^{(1)}_{y,ih}(y,z,2\omega)&=y\left(\gamma_1e^{i(K^{(1)}_{b-}(2\omega)\,r-2\omega t)}+\gamma_2e^{i(k^{(1)}_{by}(2\omega)\,r-2\omega t)}+\gamma_3e^{i(K^{(1)}_{b+}(2\omega)r-2\omega t)}\right)\\ E^{(1)}_{z,ih}(y,z,2\omega)&=z\left(\gamma_4e^{i(K^{(1)}_{b-}(2\omega)\,r-2\omega t)}+\gamma_5e^{i(k^{(1)}_{by}(2\omega)\,r-2\omega t)}+\gamma_6e^{i(K^{(1)}_{b+}(2\omega)r-2\omega t)}\right)\end{aligned} \tag{8}$$

where γ_i are some constants and $K^{(1)}_{b\pm}(2\omega)$ means $2\,K^{(1)}_{\pm}(2\omega)$.
By means of Maxwell equation

$$\nabla\times E^{(1)}_{II,\,ih}=-\frac{1}{c}\left(\frac{\partial H^{(1)}_{x,ih}}{\partial t}\right) \tag{9}$$

we obtain the following expressions for inhomogeneous contribution into the x- component of magnetic field:

$$\begin{aligned}H^{(1)}_{x,ih}(y,z,2\omega)&=\left(\frac{c}{2\omega}\right)K^{(1)}_{bZ}(2\omega)\left(\gamma_1e^{i(K^{(1)}_{b-}(2\omega)\,r-2\omega t)}-\gamma_3e^{i(K^{(1)}_{b+}(2\omega)r-2\omega t)}\right)+\\ &+\left(\frac{c}{2\omega}\right)K^{(1)}_{bY}(2\omega)\left(\gamma_4e^{i(K^{(1)}_{b-}(2\omega)\,r-2\omega t)}+\gamma_5e^{i(k^{(1)}_{by}(2\omega)\,r-2\omega t)}+\gamma_6e^{i(K^{(1)}_{b+}(2\omega)r-2\omega t)}\right)\end{aligned} \tag{10}$$

Unknown constants γ_i are determined by substitution of these formulas into the inhomogeneous wave equation

$$\nabla\times\nabla\times E^{(1)}_{II\ ih}=-\frac{1}{c}\frac{\partial^2}{\partial t^2}\left(\varepsilon^{(1)}_{2\omega}E^{(1)}_{II\ ih}\quad+4\pi P_{II\ ih}\right) \tag{11}$$

The set of constants F_α and G_α can be calculated by imposing boundary conditions on components $E^{(\alpha)}_y(2\omega)$ and $H^{(\alpha)}_x(2\omega)$ for both interfaces (air-CIGS and CIGS-Mo).
Note that components of a nonlinear polarization (NLP) is the second order polynomial on the components of the electric field of the fundamental wave and can be written in the case under consideration in the following form

$$P_i(2\omega)=\tilde{d}_{iyy}(2\omega)\left(E^{(1)}_y(\omega)\right)^2+\left(\tilde{d}_{iyz}(2\omega)+\tilde{d}_{izy}(2\omega)\right)E^{(1)}_y(\omega)E^{(1)}_z(\omega)+\tilde{d}_{izz}(2\omega)\left(E^{(1)}_z(\omega)\right)^2\quad . \tag{12}$$

In the local coordinate frame (x'', y'', z'') connected with crystalline axes of an arbitrary micro-crystal seed, we can write (in Kleinman's notation) the expression for the components of nonlinear polarization $P_{i''}(2\omega)$ for $\bar{4}2m$ point-group:

$$\begin{pmatrix} P_{x''} \\ P_{y''} \\ P_{z''} \end{pmatrix} = \begin{pmatrix} 0 & 0 & 0 & d_{14} & 0 & 0 \\ 0 & 0 & 0 & 0 & d_{25} & 0 \\ 0 & 0 & 0 & 0 & 0 & d_{36} \end{pmatrix} \cdot \begin{pmatrix} E_{x''}^2 \\ E_{y''}^2 \\ E_{z''}^2 \\ 2E_{y''}E_{z''} \\ 2E_{x''}E_{z''} \\ 2E_{x''}E_{y''} \end{pmatrix}, \qquad (13)$$

where only $d_{14} = d_{25}$, if Kleinman's conditions are valid. In the averaged medium, the same type of expressions can be written in the coordinate frame (x', y', z') connected with the orientation of the principal optic axis of the texture characterized by the set of the Euler angles (φ, ϑ, ϕ) and with some effective nonlinear coefficients $\overline{d}_{ijk}$. In the (x, y, z) coordinate frame, the components of NLP can be expressed through the $E_i^{(1)}$ components of the fundamental wave into the film, these effective $\overline{d}_{ijk}$ and known trigonometric functions of the Euler angles:

$$P_{i'}(2\omega) = \tilde{d}_{ijk}(2\omega) E_j^{(1)}(\omega) E_k^{(1)}(\omega), \qquad (14)$$

where $\tilde{d}_{ijk}(2\omega) = \overline{d}_{i'j'k'} g_{i'i} g_{j'j} g_{k'k}$ and $g_{l'l}(\varphi, \vartheta, \phi)$ are the elements of the matrix that rotate coordinate frame (x, y, z) to (x', y', z') one. Here, as usual, φ is the angle of rotation around the initial z axis (azimuth angle), ϑ is the polar angle, and ϕ is the rotation around a new orientation of the z' axis. In our case, the general expression (14) has been simplified to the form of (12).

4. Results and discussion

The calculated *p*-polarized output second harmonic signal's intensity as a function of the azimuth angle φ and determined as $I_{2\omega}(\varphi) \propto G_0 \circ G_0^*$ is presented in Fig. 3 (dashed line) in comparison with the measured one. It is shown that there is an acceptable qualitative agreement between both dependences. The calculated curve was selected by the set of adjustable parametes, such as the d_{14}/d_{36} ratio, the Euler angles $(\varphi, \vartheta, \phi)$ of the preferable orientation of the texture, and the effective thickness of the film d_f . Calculations were performed using the following input parameters for CIGS films: $n_\omega = 3.01$, $n_{2\omega} = 3.15$, $\kappa_\omega = 0,76 \cdot 10^{-4}$, $\kappa_{2\omega} = 0.30$. These constants were taken as in [8] for $CuGaSe_2$ (for 2ω, by extrapolation). The refractive and absorption indexes for Mo film $n_\omega = 3.8$, $n_{2\omega} = 3.05$, $\kappa_\omega = 3.4$, $\kappa_{2\omega} = 3.2$ were taken from the database of [9].

It was found that the axis of the preferable orientation of micro-crystals z' is about $\vartheta = 11^\circ$ relative to the surface normal. It is the c -axis of the structure (i.e. the main four-fold axis). One of the axes of the second order is rotated around this c -axis at the angle of $\phi \approx 17^\circ$. All angles are counted with respect to laboratory coordinate frame.

The d_{14}/d_{36} ratio is found to be 0.52, which indicates a sufficient deviation from the Kleinman's conditions d_{14}/d_{36} =1.0 as the wavelength is very close to the edge of the fundamental absorption. The effective thickness of the film is 2.04 μm.

It should be emphasized that the model developed and used here does not take into account the diffusion scattering of light in the film. For this reason, the model does not consider the dispersion in the orientation of micro-crystals with respect to the preferable ones. However, nearly twice wider half-width of maxima on the experimental curve in comparison with calculated one indicates the existence of dispersion.

The deviation of about 4^o -12^o observed in the location of the maxima (from 270^o or 90^o) confirms that there are slightly off-oriented areas of the film covered by the laser beam spot (about 100 μm). It means that the resulting “averaged” symmetry of the film is lower than $\bar{4}2m$.

This research has been partially supported by Russian Ministry of Education and Science.

References

[1] M.A. Contreras, B. Egaas, K. Ramanathan, J. Hiltner, A. Swartzlander, F. Hason, and R. Noufi, Progress in Photovoltaic: Research and Application **7,** 311-316 (1999).
[2] I. Repins, M.A. Contreras, B. Egaas, C. DeHart, J. Scharf, C.L. Perkins, B. To, and R. Noufi, Progress in Photovoltaic: Research and Application **16,** 235-239 (2008).
[3] G. Lüpke, Characterization of semiconductor interfaces by second-harmonic generation, Surface Science Report **35**, 75-161 (1999).
[4] E.D. Mishina, N.E. Sherstyuk, T.V. Misyuraev, A.S. Sigov, A.M. Grishin, Th. Rasing, and O.A. Aktsipetrov, Thin Solid Films **336**, 291 (1998).
[5] G. Buinitskaya, L. Kulyuk, V. Mirovitskii, E. Rusu, E. Mishina, and N. Sherstyuk, Superlattices and Microstructures **39,** 83 (2006).
[6] Sho Shirakata and Tokio Nakada, Mater. Res. Soc. Symp. Proc. **1012,** Y04-06 (2007).
[7] S.B. Zang, Su-Huai Wei, Alex Zunger, and H. Katayama-Yoshida, Phys. Rev. **B57**, 9642-9656 (1998).
[8] G.D. Boyd, H.M. Kasper, J.H. Mc Free, and F.G. Storz, IEEE J. Quant. Electr., **QE-8**, n.12, p.900-908, (1972).
[9] http://www.ioffe.ru./SVA/NSM/nk/Metals/Gif/mo.gif .